J. Microbiol. Biotechnol. (2005), **15**(3), 551–559

JOURNAL OF MICROBIOLOGY AND BIOTECHNOLOGY

Dynamic Behavior of Regulatory Elements in the Hierarchical Regulatory Network of Various Carbon Sources-Grown *Escherichia coli*

LEE, SUNG GUN, KYU SUK HWANG, AND CHEOL MIN KIM[1,2]*

Department of Chemical Engineering, College of Engineering, Pusan National University, 30 Jangjeon-dong, Geumjeong-gu, Busan 609-735, South Korea
[1]Department of Biochemistry, College of Medicine, [2]Medical Research Institute, Pusan National University, 10 Ami Dong 1-Ga, Seo-Gu, Busan 602-739, South Korea

Received: August 23, 2004
Accepted: September 21, 2004

Abstract The recent rapid increase in genomic data related to many microorganisms and the development of computational tools to accurately analyze large amounts of data have enabled us to design several kinds of simulation approaches for the complex behaviors of cells. Among these approaches, dFBA (dynamic flux balance analysis), which utilizes FBA, differential equations, and regulatory events, has correctly predicted cellular behaviors under given environmental conditions. However, until now, dFBA has centered on substrate concentration, cell growth, and gene on/off, but a detailed hierarchical structure of a regulatory network has not been taken into account. The use of Boolean rules for regulatory events in dFBA has limited the representation of interactions between specific regulatory proteins and genes and the whole transcriptional regulation mechanism with environmental change. In this paper, we adopted the operon as the basic structure, constructed a hierarchical structure for a regulatory network with defined fundamental symbols, and introduced a weight between symbols in order to solve the above problems. Finally, the total control mechanism of regulatory elements (operons, genes, effectors, etc.) with time was simulated through the linkage of dFBA with regulatory network modeling. The *lac* operon, *trp* operon, and *tna* operon in the central metabolic network of *E. coli* were chosen as the basic models for control patterns. The suggested modeling method in this study can be adopted as a basic framework to describe other transcriptional regulations, and provide biologists and engineers with useful information on transcriptional regulation mechanisms under extracellular environmental change.

Key words: Dynamic flux balance analysis, operon, transcriptional regulation

*Corresponding author
Phone: 82-51-240-7725; Fax: 82-51-248-1118;
E-mail: kimcm@pusan.ac.kr

Recent outcomes from genome research on principal microorganisms have provided systematic and intensive information at the genome level [20]. High-throughput computational analysis of this information, especially fully sequenced microbial genomes, has led to the construction of the whole biochemical pathways for cells. Logically, the next step is to study the actual biological functions of genes in microbial genomes, and eventually to construct *in silico* models for the simulation of cellular functions through biochemical pathways on computer.

Firstly, it has been observed both experimentally and computationally that genes in microbial genomes tend to form modular functional units that are conserved and coordinately regulated during evolution [6, 22, 27]. A cluster of these genes is called an operon [8]. Operon structures are known to be an important family among these conserved functionally related genomic units. Moreover, these units often appear in multiple genomes and perform highly compartmentalized activities in biochemical pathways [35]. Experimental detection and confirmation of these operons is time-consuming and relatively difficult to perform in the laboratory due to a high-throughput process. To overcome this problem, several computational methods for modeling and predicting operons in *E. coli* as a model organism [34] have been suggested. Now, regulons, operons, regulatory proteins, structural genes, effectors, and metabolic pathways related to *E. coli* can easily be researched through RegulonDB [11] and EcoCyc [12] on the Web.

Secondly, the regulatory and metabolic models that are based on constructed biological pathways have had beneficial effects on several fields. Microarrays have been developed to analyze gene expression patterns; they are necessary to predict intracelluar transcription and transcriptional regulation under given environmental conditions [2]. These models have also been very useful in metabolic engineering. This

is the reason why metabolic engineers can produce the desired biochemical species [9, 10, 16, 17, 31], by using the models. This usefulness induces many research groups to suggest several approaches to analyze metabolic and regulatory models with simulation. The approaches, using a qualitative model, deal well with the lack of information to describe cellular metabolism or quantitative data in molecular biology. However, they often generate incorrect results and behaviors due to combinatorial explosion [19, 21, 28]. Another type of model uses the kinetic theory for studying catabolite repression and diauxic growth on glucose and lactose in *E. coli* [15, 33]. This method also has a disadvantage that requires detailed kinetic and concentration data on enzymes.

When there is a lack of detailed kinetic information, FBA (flux balance analysis) can accurately analyze metabolic capabilities, cell growth rate, metabolic byproducts, substrate concentrations, and important reactions related to achieving a desired production [29]. Information required for the analysis is stoichiometry of metabolic pathways, metabolic requirements, and fundamental physicochemical constraints. This information is well known and easily obtainable. FBA can also be used for the dynamic prediction of cell growth, metabolic byproduct secretion, and substrate concentrations [30, 31].

Recently, researchers have attempted to incorporate regulatory constraints in dFBA, as previous studies did not consider them, despite that the constraints have a significant effect on the behavior of an organism. dFBA is divided into two formulations: dynamic optimization approach (DOA) and static optimization approach (SOA) [20]. The dFBA method proposed by Varma and Palsson [30] belongs to SOA without rate-of-change constraints on the metabolic fluxes. In this paper, this approach was adopted. The regulatory constraints in dFBA can be represented with the logic method [2]. Therefore, dFBA with the logic method has been used to quantitatively predict diauxic growth in *E. coli*.

The logic method uses the equations represented by the production rule (If-Then rules) and Boolean logic. This Boolean rule-based system has the advantage to describe well the causal relation between two events and to convert states in any condition to rules. However, Boolean rule has some problems, such as difficulty to represent interactions with specific regulatory proteins and genes, since it is a binary (true, false) system [4]. It also has the disadvantage of not knowing the total operon and gene control mechanism due to its difficulty to track the application of rules [32].

In this paper, in order to solve these disadvantages, we introduced (I) a weight for a degree of connectivity between regulatory elements (regulatory protein, gene, effector, etc.) in the digraph and (II) a hierarchical structure for a regulatory network that is composed of modeled operons with Boolean symbols as a basic structure, and (III) simulated the total control mechanism of regulatory elements with time through the linkage of a constructed regulatory network and dFBA. These dynamic transcriptional regulation simulations can provide biologists and engineers with useful information on the control mechanisms of regulatory elements to extracellular environmental change.

MATERIALS AND METHODS

Modeling and Construction of Two Modules

Graph theory and Boolean symbols were introduced to simulate the transcriptional regulation mechanism with environmental change. The hierarchical structure for the regulatory network was built by operon units. Each operon organized in the form of a hierarchical structure is modeled with defined fundamental modeling symbols, and RMM (regulatory modeling module) was built. Dynamic transcriptional regulation was performed through the linkage of RMM and dFBAM (dynamic flux balance analysis module). The *lac* operon, *trp* operon, and *tna* operon were chosen as basic examples for modeling illustration.

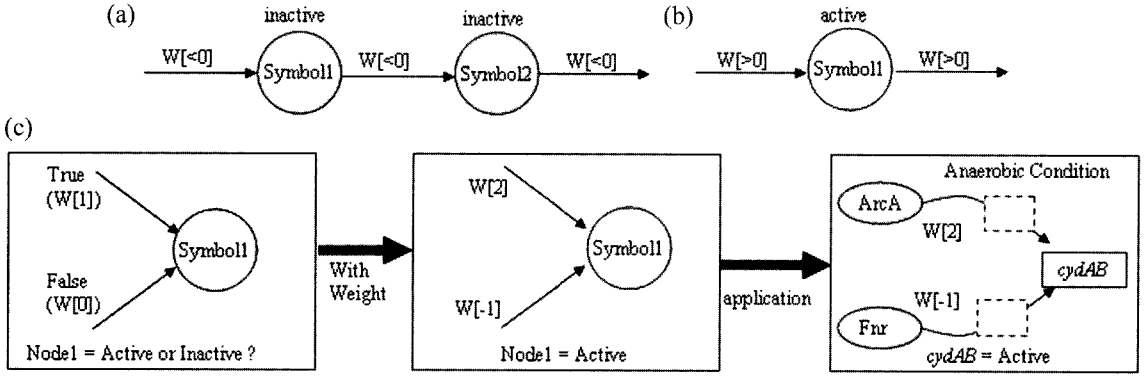

Fig. 1. Symbols change to weight.
(a) Inactive condition of symbol. (b) Active condition of symbol. (c) Weight application to the binary system.

Fundamental Modeling Symbols

Operons in RMM consisted of symbols and weights. Modeling symbols were divided into biological symbols for regulation and non-biological symbols for weight. Promoter, not gate, and operator formed a cluster that acted as gene transcription. Arc represented the existence of causal relationship among symbols and was used for propagation of weight. Weight was used to determine the active/inactive state of a symbol and can also indicate a degree of connectivity between symbols. It can be effectively used in conditions that are not represented with a binary system.

In Fig. 1(c), a binary system can not deal with a situation where true and false events occur at the same time. However, by adding a degree of connectivity to weight, the problem can be solved. In fact, the situation was generated at the relation Fnr→*cydAB* and ArcA→*cydAB* under anaerobic conditions. Fnr acted as a repressor and ArcA as an activator to *cydAB* [5, 11, 26].

Basic Operon Modeling

Operons were modeled, using fundamental symbols (Table 1). Modeled operons were composed of five symbols: P (promoter), RP (regulatory protein), O (operator), SG (structural genes), SW (switch, on/off), and have a positive control mode and a negative control mode by pattern governed genes. The "not gate" in an operon became active under a negative control mode.

Table 1. Fundamental modeling symbols.

Function	Symbol
Operator	O
Structural gene	SG
Promoter (RNA polymerase)	P
Regulatory protein (or transcription factor)	RP
Effector (inducer, repressor)	E
Gene transcription negative control	O NG P
positive control	O NG P
Weight distributor	
And gate	
Not gate	
Switch for operon	ON OFF
Node state active/inactive	

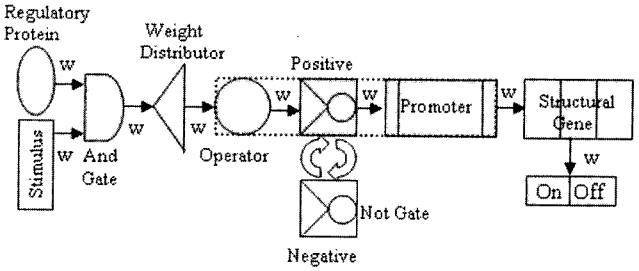

Fig. 2. Operon structure and modeling with biological and non-biological symbols.

The state value of a node was 1 or 0, which was determined by the propagation of weight and the Boolean symbols for weight, through an arc. If weight was over 1 or below 0, it was regarded as 1 or 0 at the step to determine symbol state. In Fig. 2, O can not have a direct influence on SG, but P can have an influence on the state of SG. Eventually, if SG becomes active, front symbols have to orderly be active for active SG. From this point of view, an operon modeled with symbols has a control mechanism and shows the entire regulation procedure of gene expression.

The *lac* operon modeling had a positive control mode (Fig. 3A) and a negative control mode (Fig. 3B1) [1]. In a negative control mode, not gate existed between S2 and RP2, since lactose in S2 obstructed the function of LacI, therefore, not gate between O2 and P2 became active. In a positive control mode, not gate existed between S1 and E1, since glucose in S1 made the concentration level of cAMP low, therefore, not gate between O2 and P2 became inactive.

The *trp* and *tna* operons, related to the synthesis and degradation of amino acids, are very different from the *lac* operon, thus allowing cells to use particular carbon sources.

A gene transcription in *trp* operon modeling (Fig. 3C) corresponded to a negative control mode, and not gate between O3 and P3 became active. However, not gate between S4 and RP4 did not exist, since tryptophan acted as a co-repressor.

A gene transcription in *tna* operon modeling (Fig. 3B2) corresponded to a positive control mode. So, not gate between O2 and P2 became active, but not gate between S3 and RP3 did not exist, since tryptophan as a stimulus made *tna* regulatory protein active [7, 14]. The *tna* operon turned on when tryptophan was used as an alternate carbon energy source and was opposite to the *trp* operon in function [13].

Construction of RMM

Hierarchical Structure Construction Within a Global Regulatory Network. A global regulatory network as a part of RMM organized by modeled operons can intuitively show how a set of genes are regulated (Fig. 3). This network

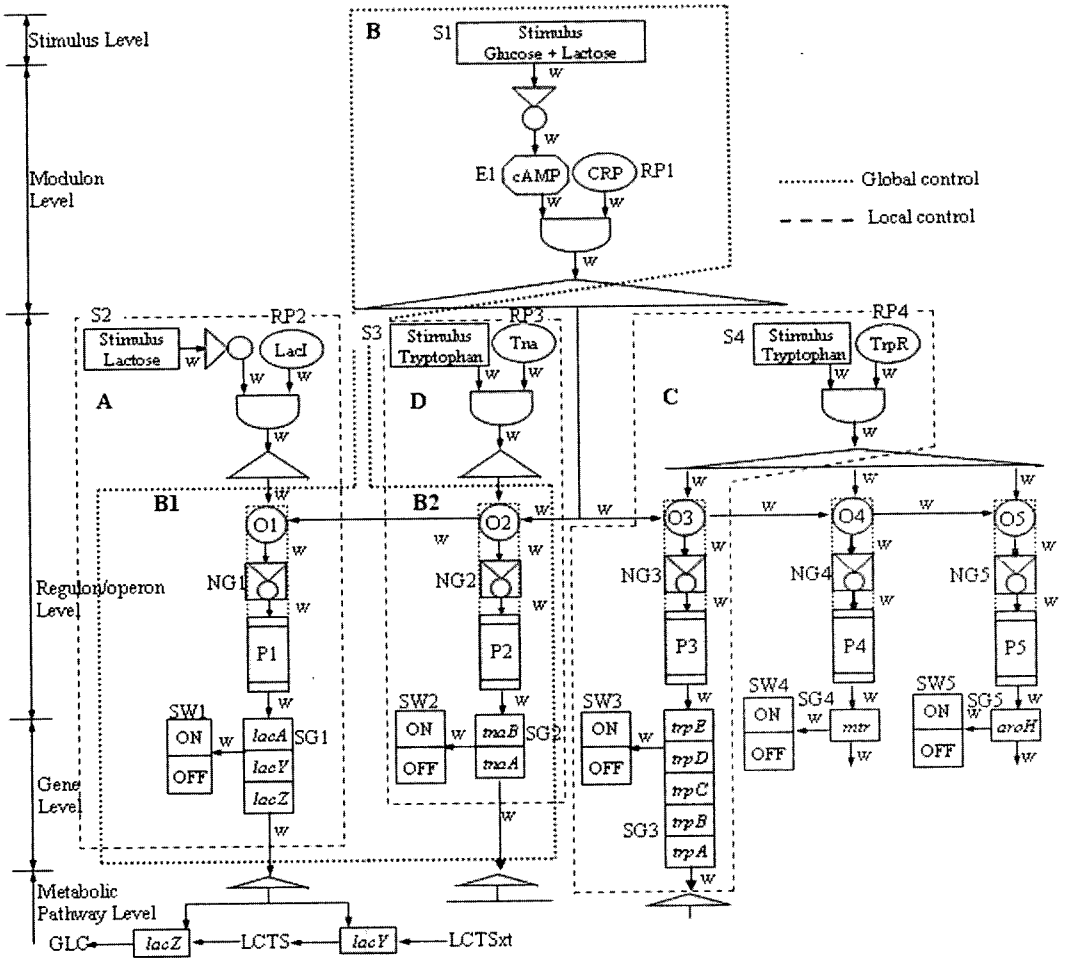

Fig. 3. Hierarchical structure of the global regulatory network.
A: Negative *lac* operon. B1: Positive *lac* operon. C: *trp* operon. B2 and D: *tna* operon.

can be hierarchically divided into stimulus, modulon, regulon/operon, gene level, and metabolic pathway level. The stimulus level is a simple environmental change. The modulon level responds to extracellular environmental change and coordinately regulates regulons/operons with global regulatory protein. The regulon/operon level directly governs a set of operons or a set of genes [25]. The gene level indicates active/inactive of genes regulated by an operon. These genes stimulate reactions in the metabolic pathway level, which synthesizes or decays metabolites for cellular growth.

Construction of dFBAM

Central Metabolic Pathway of *E. coli*. In this research, the previously studied core metabolic network of *E. coli* [19] was taken and expanded. We found 21 regulatory proteins controlling genes that are related to the central metabolic pathway, 19 operons containing structural genes that were comprised of more than two genes, 87 genes (71.9%, 87/121) regulated by regulatory protein, and 66 genes (75.9%, 66/87) controlled by more than two regulatory proteins among genes that are governed by regulatory proteins in the central metabolic pathway.

Dynamic Flux Balance Analysis

Using FBA and iterative algorithm [30, 31], dFBA can quantitatively predict cell density and metabolic byproduct. In this study, dFBA was a static optimization-based analysis that did not contain rate-of-constraints [20].

To quantitatively predict cellular behavior, the batch time was first divided into small time intervals (Δt). Given initial values, FBA was utilized to estimate actual substrate uptake, growth rate, and byproduct [14, 26, 27]. With these data from FBA, concentrations for the next time step were repeatedly calculated from a standard differential equation (Appendix) through an iterative algorithm. Lastly, by integrating small time intervals, the variation of concentration over all the intervals was predicted. During the integration, there was the assumption that flux is constant in an interval [30].

Table 2. Regulatory proteins and regulated genes in the central metabolic pathway in *E. coli*.

Regulatory proteins	Genes controlled by a regulatory protein	A set of genes controlled by a regulatory protein
ArcA, CRP, DcuR, FadR, FIS, Fnr, FruR, GalR, IclR, IHF, LacI, MarA, Mlc, NarL, Pdh, RbsR, Rob, RpiR, RpoN, SoxS, TrpR	*acnA*, *acs*, *adhE*, *dctA*, *fumA*, *fumC*, *glpD*, *icdA*, *mdh*, *ndh*, *pgk*, *ppsA*, *pykF*, *zwf*	*aceBAK*, *cydAB*, *cyoABCDE*, *dcuB-fumB*, *fdnGHI*, *focA-pflB*, *frdABCD*, *galETKM*, *glpACB*, *glpFK*, *lacZYA*, *nuoABEF-GHIJKLMN*, *pdhR-aceEF-lpdA*, *ptsGHI-crr*, *rbsABCD*, *rpiB-serA*, *sdhABCD-sucAB*, *tnaAB*, *trpEDCBA*

RESULTS

Linkage of RMM and dFBAM

A simulation of dynamic regulatory elements in the hierarchical regulation network was preformed through linkage of RMM and dFBAM. RMM provides information on interactions among elements in a hierarchical regulatory structure, delay time, and constraints for simulation.

Delay time is a period where a gene becomes active from an inactive state, and an enzyme is synthesized and degraded. The time consists of reaction time, transcription time, and protein synthesis/degradation time. The average synthesis and degradation times are equal at steady state [2]. In this study, we set 0.5 h as the total delay time; reaction time between cAMP and CRP was set at 1 sec due to a fast reaction; transcription time was *lacAYZ*=2 min; *tnaAB*=1 min by the length of gene sequence [25]; and protein synthesis/degradation time was *lacAYZ*=28 min, *tnaAB*=29 min.

dFBAM provides information on substrate concentrations and time profiles. The concentration changes in substrates happen just after an operon turns on, and delay time is added by the variation in an operon state, from off to on. Time profile includes this delay time. Since the concentration change represents an extracellular environment, they can alter the on/off state of an operon. By following the above procedure, linkage of RMM and dFBAM could lead to a dynamic simulation of the total regulatory elements and mechanism with environment conditions.

Parameters for Simulation

The modeling suggested in this paper was illustrated by simulating regulatory elements with a hierarchical structure of regulatory network (Fig. 3), a central metabolic pathway [24], and parameters. LINGO (Lindo Systems Inc.), as a software tool for optimization, was used to identify optimal flux distribution in the central metabolic network of *E. coli*. Matlab (The MathWorks, Inc.) was also used to calculate and represent concentration changes and operons on/off with time. As parameters for dFBA, initial condition (biomass: 0.011 g/l; glucose: 1.6 mM; lactose: 5.8 mM; tryptophan 1.0 mM; delay time: 0.5 h) and uptake rate constraints (glucose: 6.5 mM/g·DCW·h; lactose: 3.0 mM/g·DCW·h; tryptophan: 2.0 mM/g·DCW·h, estimated; and oxygen: 15.0 mM/g·DCW·h) were obtained from the literature [3].

Case Study 1. Glucose and Lactose in the Medium

When both glucose and lactose existed in the extracellular environment, S1 of the stimulus level located in the highest part of RMM was activated. Weight became W[1] due to the existence of glucose. The value was propagated through arc. At the modulon level, the value varied from W[1] to W[0] through not gate, and cAMP was inactivated. This shows that glucose makes the concentration level of cAMP low and the cAMP/CRP complex can not be produced. W[0] from the above result was transferred to the regulon/operon level. At the regulon/operon level, O1 was inactivated by W[0]. NG1 was also inactivated due to choosing a positive control mode by S1. W[0] from NG1 allowed P1 to be inactive, and finally, gene transcription was turned off. At the gene level, *lacAYZ* was inactivated by gene transcription weight value, W[0], and *lac* operon was turned off. This led to preventing lactose metabolism at the metabolic pathway level. The inactive state of *lacAYZ* was maintained until dFBAM returned to the [0] value, which the glucose concentration was at. When the glucose concentration was [0], only lactose was present in S1. So, W[0] was sent to the modulon level through arc. W[0] was varied to W[1] through not gate and E1, and RP1 became active since glucose was not present. The weight value of the modulon level was, as mentioned above, propagated to the lower levels step by step, and *lacAYZ* was used for lactose metabolism at the metabolic pathway. The metabolism was working until dFBAM returned to lactose concentration [0]. The [0] value made *lac* operon off again. The off time was also obtained from dFBAM.

The active/inactive state of the regulatory elements with time [Fig. 4(b)] shows well that *E. coli* preferred glucose as a carbon source and did not metabolize lactose until all the glucose was used up [23]. The total time can be divided into three parts: glucose metabolism, transport protein synthesis for the lactose metabolism, lactose metabolism. To 0 h from 4.4 h, the glucose metabolism part, only RP1 was activated and the others, E1, O1, NG1, P1, SG1, and SW1, were inactivated. S2 and RP2 related to local control were N (none) due to global control. To 4.4 h from 4.9 h, E1, O1, P1, SG1, and SW1, were activated for lactose as an alternate carbon source, and to 8.5 h from 4.9 h, lactose was metabolized.

Case Study 2. Glucose and Tryptophan in the Medium

When both glucose and tryptophan were present, S1 and S4 were activated at the same time. Performing the

same mechanism as in Case Study 1, a global control mode by the activated S1 allowed *tnaAB* to be inactive. The *tna* operon off state was maintained until dFBAM returned to the [0] value in glucose concentration. When only tryptophan was present in S1, the weight of S1 was W[0]. W[0] was converted into W[1] through not gate. Gene transcription in the regulon/operon level became active by W[1]. Eventually, the gene level and metabolic pathway level orderly became active and tryptophan was metabolized.

The active state of S4 began at the regulon/operon level and corresponded to a local control. By the activation of both S4 and RP4, W[1] was sent to O3. Activation of O3 means binding tryptophan and the *TrpR* regulatory protein to the operator. Due to a negative control mode, NG3 became active and varied from W[1] to W[0]. W[0] from the regulon/operon level was propagated to the gene level. Finally, at the metabolic pathway level, *trpEDCBA* became inactive, and the trp operon off was continuously in off state, due to the existence of tryptophan.

(a)

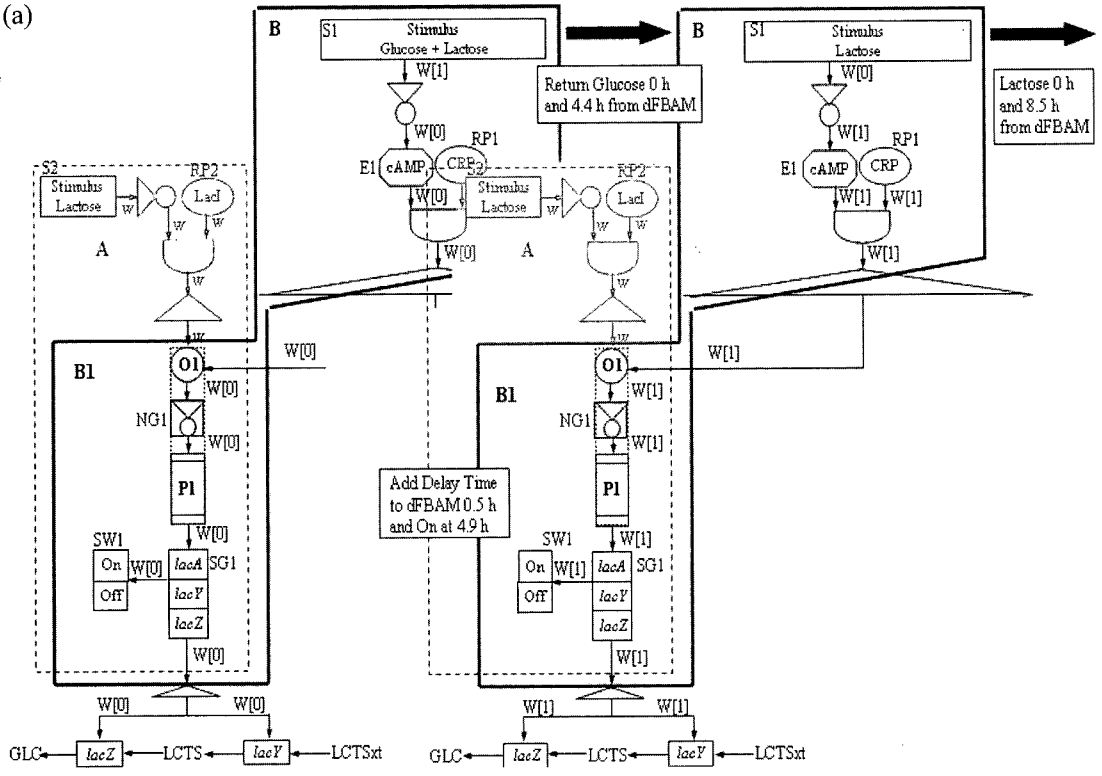

(b)

Time (h)		S1	S2	E1	RP1	RP2	O1	NG1	P1	SG1	SW1
0		1	N	0	1	N	0	0	0	0	0
4.4		0	N	0	1	N	0	0	0	0	0
4.9	1 sec	0	N	1	1	N	0	0	0	0	0
	2 min	0	N	1	1	N	1	0	1	0	0
	28 min	0	N	1	1	N	1	0	1	1	1
8.5		0	N	0	0	N	0	0	0	0	0

(c)

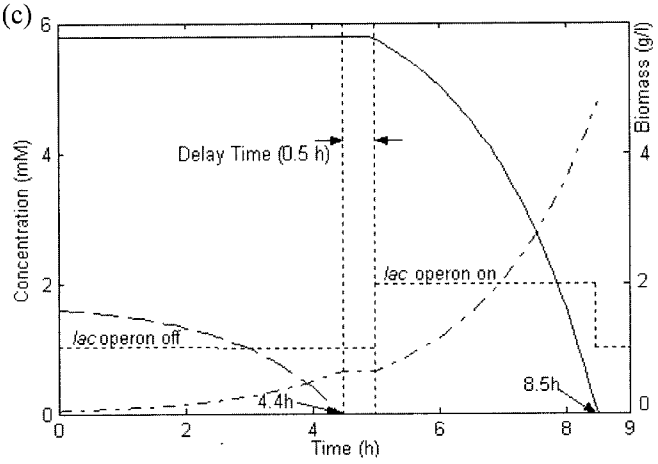

Fig. 4. Dynamic gene regulation for two carbon sources.
(a) Weight propagation in digraph. (b) Active/inactive regulatory elements with time. 1: Activation; 0: inactivation; N: none. (c) Metabolite concentration change and lac operon on/off simulation. (—) glucose; (—) lactose; (– –) biomass.

(a)

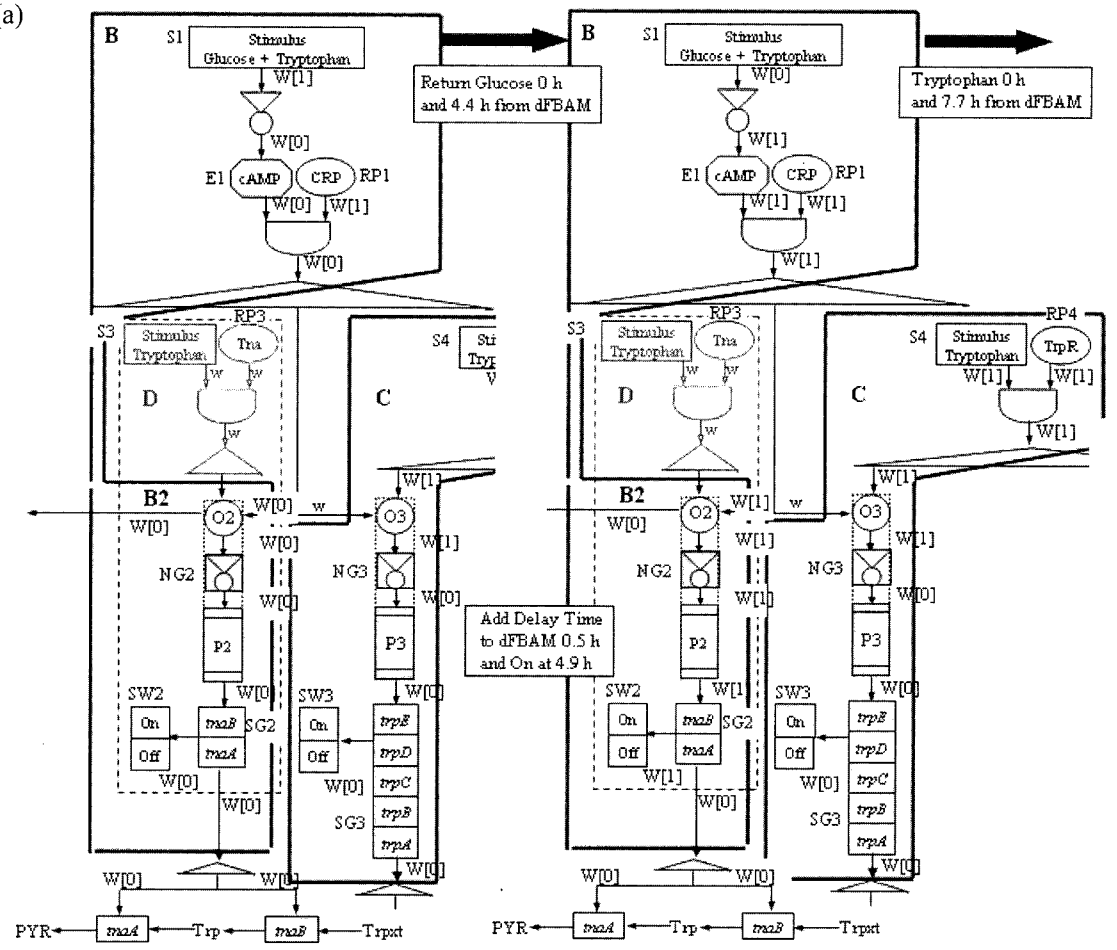

(b)

Time (h)		S1	S3	S4	E1	RP1	RP3	RP4	O2	O3	NG2	NG3
0		1	N	1	0	1	N	1	0	1	0	1
4.4		0	N	1	0	1	N	1	0	1	0	1
4.9	1 sec	0	N	1	1	1	N	1	0	1	0	1
	1 min	0	N	1	1	1	N	1	1	1	0	1
	29 min	0	N	1	1	1	N	1	1	1	0	1
7.7		0	N	0	0	0	N	0	0	0	0	0

P2	P3	SG2	SG3	SW2	SW3
0	0	0	0	0	0
0	0	0	0	0	0
0	0	0	0	0	0
1	0	0	0	0	0
1	0	1	0	1	0
0	0	0	0	0	0

(c)

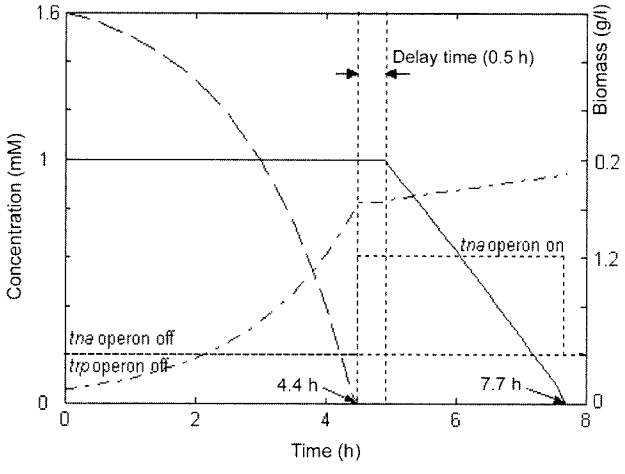

Fig. 5. Dynamic gene regulation for two carbon sources, glucose-tryptophan.
(a) Weight propagation in digraph. (b) Active/inactive regulatory elements with time. 1: Activation; 0: inactivation; N: none. (c) Metabolite concentration change and two operons on/off simulation. (—) glucose; (—) tryptophan; (- -) biomass.

Figure 4b shows that when both glucose and tryptophan in S1 were present, *E. coli* also preferred glucose to tryptophan as an alternate carbon energy source. Glucose metabolism, transport protein synthesis for tryptophan, and tryptophan metabolism are divided. To 0 h from 4.4 h, glucose metabolism, S4, RP4, O3, and NG3 in addition to S1 and RP1 became active by tryptophan. These results showed that global and local control was preformed together. However, S3 and RP3 in another local control became N (none). To 4.4 h from 4.9 h, E1, O1, P1, SG1, and SW1 were activated for tryptophan metabolism. To 7.7 h from 4.9 h, tryptophan was metabolized. During the period, S4, RP4, O3, and NG3 continuously became active in order not to produce tryptophan.

DISCUSSION

In this paper, we have built a hierarchical regulatory network with basic operon models in order to represent gene regulation mechanisms in the central metabolic pathway of *E. coli* and introduced a weight for a degree of connectivity. Linking RMM and dFBAM, dynamic regulatory elements for gene expression have been simulated.

Each of the operons in RMM can show precedent conditions and a flow of entire control for gene expression. Figure 4(a) and Fig. 5(a) illustrate the conditions and regulatory procedures that *lacZYA* in the *lac* operon, *tnaAB* in the *tna* operon, and *trpEDCBA* in the *trp* operon become active. Here, active or inactive states of genes were determined by regulatory elements and effectors responding to extracellular environmental changes with time. The carbon source was preferentially metabolized, as a stimulus in the upper or lower level was chosen and the operons or genes were globally or locally controlled.

Genes regulated by more than a regulatory protein were 71.9% of the genes in the central metabolic pathway of *E. coli*. This result shows that the central metabolic pathway is sensitive to environmental changes.

The linkage of RMM and dFBA is capable of making predictions about gene regulation, on/off states of operons, and concentration changes of the carbon source with time. These examples are also shown in Fig. 4 and Fig. 5. The time profiles for glucose and lactose concentrations were very similar to ones in a previous paper [15]. In our results, when the off state of an operon was converted into the on state, delay time was applied. The concentrations of lactose and tryptophan as a carbon source were reduced in situations where each of the operons was on. If the operon were off, a decrease in the carbon source did not happen. From this point of view, recognition of stimulus, modulon, and regulon governing operons coordinately can be very important, since an operon can become a constraint. In Fig. 5(c), the linear decrease of tryptophan concentration occurs since the growth rate of the cells is very low during metabolizing tryptophan. Another similar response, shown as a linear line, happens in the growth on acetate reutilization [3, 30].

Operons related to amino acid synthesis/degradation have the opposite effect on each other. Interaction between the *tna* operon and *trp* operon serves as an example. Each different mechanism is involved, therefore, these operons do not turn on at the same time. In simulation results, the *tna* operon turned on/off with a global control and the *trp* operon turned on/off with a local control.

In summary, in order to solve problems that have not been considered or generated in previous Boolean rule-based dFBA, (I) a weight was introduced, (II) a hierarchical structure for a regulatory network including Boolean symbols was constructed, and (III) dynamic regulatory elements and mechanisms required for gene expression were simulated. These detailed simulation results can provide biologists and engineers with useful information on cellular metabolism regulation, regulatory proteins, genes, and effectors.

Acknowledgment

This work was supported by Brain Korea 21 Project in 2003.

APPENDIX

We used the following equations for prediction of substrate concentration.

$$S = So + \frac{Su}{\mu}(Xo - X)$$

$$X = Xo * e^{\mu \cdot \Delta t}$$

So : Initial substrate concentration
S : Substrate concentration predicted for the next time step
Su : Uptake rate constraints
Xo : Initial biomass
X : Initial biomass
μ : Growth rate
Δt : Small time interval

REFERENCES

1. Adhya, S. 1996. The *lac* and *gal* operons today, pp. 181–200. *In* E. C. C. Lin and A. Simon Lynch (eds.), *Regulation of Gene Expression in Escherichia coli.* Chapman & Hall, New York, U.S.A.
2. Covert, M. W., C. H. Schilling, and B. O. Palsson. 2001. Regulation of gene expression in flux balance models of metabolism. *J. Theor. Biol.* **213:** 73–88.

3. Covert, M. W. and B. O. Palsson. 2002. Transcriptional regulation in constraints-based metabolic models of *Escherichia coli*. *J. Biol. Chem.* **277:** 28058–28064.
4. Covert, M. W., E. M. Knight, J. L. Reed, M. J. Herrgard, and B. O. Palsson. 2004. Integrating high-throughput and computational data elucidates bacterial networks. *Nature* **429:** 92–96.
5. Cotter, P. A. and R. P. Gunsalus. 1992. Contribution of the Fnr and ArcA gene products in coordinate regulation of cytochrome o and d oxidase (*cyoABCDE* and *cydAB*) genes in *Escherichia coli*. *FEMS Microbiol. Lett.* **70:** 31–36.
6. Ettema, T., J. van der Oost, and M. Huynen. 2001. Modularity in the gain microbial genomes. *Trends Genet.* **17:** 485–487.
7. Feng, G. and C. Yanofsky. 2001. Reproducing *tna* operon regulation *in vitro* in an S-30 system. *J. Biol. Chem.* **276:** 1974–1983.
8. Glick, B. R. and J. J. Pasternak. 1998. *Molecular Biotechnology*, pp. 35–38. 2nd Ed. ASM Press, Washington, DC, U.S.A.
9. Hong, S. H. and S. Y. Lee. 2000. Metabolic flux distribution in a metabolically engineered *Escherichia coli* strain producing succinic acid. *J. Microbiol. Biotechnol.* **10:** 496–501.
10. Hong, S. H., S. Y. Moon, and S. Y. Lee. 2003. Prediction of maximum yields of metabolites and optimal pathways for their production by metabolic flux analysis. *J. Microbiol. Biotechnol.* **13:** 571–577.
11. Huerta, A. M., H. Salgado, D. Thieffry, and J. Collado-Vides. 1998. RegulonDB: A database on transcriptional regulation in *Escherichia coli*. *Nucleic Acids Res.* **26:** 55–59.
12. Karp, P. D., R. Monica, S. Milton, T. P. Ian, M. P. Suzanne, and P. T. Alida. 2000. The EcoCyc and MetaCyc databases. *Nucleic Acids Res.* **28:** 56–59.
13. Kazarinoff, M. N. and E. E. Snell, 1977. Essential arginine residues in *tryptophanase* from *Escherichia coli*. *J. Biol. Chem.* **252:** 7598–7602.
14. Konan, V. K. and C. Yanofsky. 2000. Rho-dependent transcription termination in the *tna* operon of *Escherichia coli*: Roles of the boxA sequence and the rut site. *J. Bacteriol.* **182:** 3981–3988.
15. Kremling, A., K. Bettenbrock, B. Laube, J. W. Lengeler, and E. D. Gilles. 2001. The organization of metabolic reaction networks: Application for diauxic growth on glucose and lactose. *Metab. Eng.* **3:** 362–379.
16. Lee, J. W., A. Goel, M. M. Ataai, and M. M. Domach. 2002. Flux regulation patterns and energy audit of *E. coli* B/r and K-12. *J. Microbiol. Biotechnol.* **12:** 248–258.
17. Lee, T. H., M. Y. Kim, Y. W. Ryu, and J. H. Seo. 2001. Estimation of theoretical yield for ethanol production from D-xylose by recombinant *Saccharomyces cerevisiae* using metabolic pathway synthesis algorithm. *J. Microbiol. Biotechnol.* **11:** 384–388.
18. Lee, S. Y. and Papoutsakis. 1999. *Metabolic Flux Balance Analysis*, pp. 13–57. Marcel Dekker, New York, U.S.A.
19. MacAdams, H. H. and L. Shapiro. 1995. Circuit simulation of genetic networks. *Science* **269:** 650–656.
20. Mahadevan, R., J. S. Edwards, and J. D. Francis. 2002. Dynamic flux balance analysis of diauxic growth in *Escherichia coli*. *Biophys. J.* **83:** 1331–1340.
21. Meyers, S. and P. Friedland. 1984. Knowledge-based simulation of genetic regulation in bacteriophage lambda. *Nucleic Acids Res.* **12:** 1–9.
22. Overbeek, R., M. Fonstein, M. D'Souza, G. D. Pusch, and N. Maltsev. 1999. The use of gene clusters to infer functional coupling. *Proc. Natl. Acad. Sci. USA* **96:** 2896–2901.
23. Saier, M. H. J., T. M. Ramseier, and J. Reiszer. 1996. Regulation of carbon utilization, pp. 1325–1343. *In* F. C. Neidhardt (ed.), *Escherichia coli and Salmonella: Cellular and Molecular Biology*, vol. 1. ASM Press, Washington, D.C.
24. Schilling, C. H., J. S. Edwards, D. Letscher, and B. O. Palsson. 2000. Combining pathway analysis with flux balance analysis for the comprehensive study of metabolic systems. *Biotechnol. Bioeng.* **71:** 286–306.
25. Stephanopoulos, G. N., A. A. Aristidou, and J. Nielsen. 1998. *Metabolic Engineering: Principles and Methodologies*, pp. 180–193. Academic Press, London, U.K.
26. Shen-Orr, S. S., R. Milo, S. Mangan, and U. Alon. 2002. Network motifs in the transcriptional regulation network of *Escherichia coli*. *Nat. Genet.* **31:** 64–68.
27. Tamames, J., G. Casari, C. Ouzounis, and A. Valencia. 1997. Conserved cluster of functionally related genes in two bacterial genomes. *J. Mol. Evol.* **44:** 66–73.
28. Tomita, M., K. Hashimoto, K. Takahashi, T. S. Shimizu, Y. Matsuzaki, F. Miyoshi, K. Saito, S. Yugi, K. Tanida, J. C. Venter, and C. A. Hutchison III. 1999. E-Cell: Software environment for whole-cell simulation. *Bioinformatics* **15:** 72–84.
29. Varma, A., B. W. Boesch, and B. O. Palsson. 1993. Stoichiometric interpretation of *Escherichia coli* glucose catabolism under various oxygenation rates. *Appl. Environ. Microbiol.* **59:** 2465–2473.
30. Varma, A. and B. O. Palsson. 1994. Stoichiometric flux balance models quantitatively predict growth and metabolic by-product secretion in wild type *Escherichia coli* W3110. *Appl. Environ. Microbol.* **60:** 3724–3731.
31. Varma, A. and B. O. Palsson. 1994. Metabolic flux balancing: Basic concepts, scientific and practical use. *Nat. Biotech.* **12:** 994–998.
32. Winston, P. H. 1992. *Artificial Intelligence*, pp. 119–137. 3th Ed. Addison Wesley, Massachusetts, U.S.A.
33. Wong, P., S. Gladney, and J. D. Keasling. 1997. Mathematical model of the *lac* operon: Inducer exclusion, catabolite repression, and diauxic growth on glucose and lactose. *Biotechnol. Progr.* **13:** 132–143.
34. Yada, T., M. Nakao, Y. Totoki, and K. Nakai. 1999. Modeling and predicting transcriptional units of *Escherichia coli* genes using hidden Markov models. *Bioinformatics* **15:** 987–993.
35. Zheng, Y., J. D. Szustakowski, L. Fortnow, R. J. Roberts, and S. Kasif. 2002. Computational identification of operons in microbial genomes. *Genome Res.* **12:** 1221–1230.